**Proceedings of the XVIII ECSMGE 2024**
GEOTECHNICAL ENGINEERING CHALLENGES
TO MEET CURRENT AND EMERGING NEEDS OF SOCIETY

ISBN 978-1-032-54816-6
DOI 10.1201/9781003431749-494


ECSMGE 24
XVIII EUROPEAN CONFERENCE ON SOIL MECHANICS AND GEOTECHNICAL ENGINEERING

# Consideration of the variable contact geometry between the drum and the soil surface in vibratory roller compaction

## Prise en compte de la géométrie de contact variable entre le cylindre et la surface du sol lors du compactage par rouleau vibrant

J. Pistrol*, M. Hager, D. Adam
*TU Wien, Institute of Geotechnics, Vienna, Austria*

F. Kopf
*FCP - Fritsch, Chiari & Partner ZT GmbH, Vienna, Austria*

**johannes.pistrol@tuwien.ac.at*

**ABSTRACT**: The paper presents a comparatively simple mechanical model, which describes the dynamic interaction between the drum of a vibratory roller and the underlying soil during compaction. The main non-linearities of the dynamic system are the continuously varying contact conditions and geometry between the drum and the subgrade as well as the curved drum geometry. As the drum penetrates the soil during the loading phase, the contact area between the two contact partners increases, which in turn affects the resulting soil reaction force and influences the motion behaviour of the drum at the same time. Moreover, a periodic loss of contact between drum and soil during the unloading phase may occur, and the two subsystems move separately and independently from each other for a short period of time. The model introduced in the paper allows for a consideration of the challenging contact conditions and the variable drum contact geometry. Moreover, it enables the consideration of varying soil resistance as a result of the changing contact conditions. The model is tested on the example of a typical vibratory roller and the results are compared to a simulation with a constant contact geometry between drum and soil. The presented findings allow for a more accurate consideration of the actual contact conditions between the drum of a vibratory roller and the soil and are considered valuable for the further development of measurement values of Intelligent Compaction.

**RÉSUMÉ**: Cet article présente un modèle mécanique relativement simple, qui décrit l'interaction dynamique entre le tambour d'un rouleau vibrant et le sol sous-jacent pendant le compactage. Les principales non-linéarités du système dynamique sont les conditions de contact et la géométrie continuellement variables entre le cylindre et le sol de fondation, ainsi que la géométrie incurvée du cylindre. Au fur et à mesure que le cylindre pénètre dans le sol pendant la phase de chargement, la surface de contact entre les deux partenaires augmente, ce qui affecte la force de réaction du sol et le comportement de mouvement du cylindre. En outre, une perte de contact périodique entre le tambour et le sol pendant la phase de déchargement peut se produire, et les deux sous-systèmes se déplacent séparément et indépendamment l'un de l'autre pendant une courte période. Le modèle présenté dans cet article permet de prendre en compte les conditions de contact difficiles et la géométrie variable du contact entre le tambour et le sol. En outre, il permet de prendre en compte la résistance variable du sol résultant de l'évolution des conditions de contact. Le modèle est testé sur l'exemple d'un rouleau vibrant typique et les résultats sont comparés à une simulation avec une géométrie de contact constante entre le tambour et le sol. Les résultats présentés permettent une prise en compte plus précise des conditions de contact réelles entre le tambour d'un rouleau vibrant et le sol et sont considérés comme précieux pour le développement ultérieur des valeurs de mesure du compactage intelligent.

**Keywords:** Roller compaction; soil dynamics; intelligent compaction; non-destructive testing.

## 1 INTRODUCTION

This paper presents a comparatively simple semi-analytical vibratory roller-soil simulation model to describe the interaction system, characterized by its challenging contact conditions. Previous models consider, if at all, only a constant geometry of the contact area between drum and soil (Adam, 1996). However, the width of the contact area increases during the loading phase, making the drum contact width a variable parameter. The presented model can account for this variability of the drum contact width in the loading phase of vibratory roller compaction. The model is part of an ongoing research project to develop a novel Intelligent compaction meter value (ICMV) for roller compaction (Pistrol et al., 2023).

## 2 MECHANICAL MODEL

### 2.1 Modelling of the roller subsystem

The cylindrically curved drum of the roller is excited at a specific frequency $f$ by an unbalance, which is mounted on a drive shaft in the axis of the drum. The resulting vibration of the drum yields a predominantly vertically directed loading of the soil.

The drum is connected to the frame of the roller using rubber buffers. If the rubber buffers and the frame are suitably designed, the frame and drum can be regarded as largely decoupled. Therefore, the influence of the frame on the motion behaviour of the drum is limited to its dead weight ($m_f g$) and the roller subsystem is reduced to a single degree of freedom with the position coordinate $z_1$ (see Figure 1).

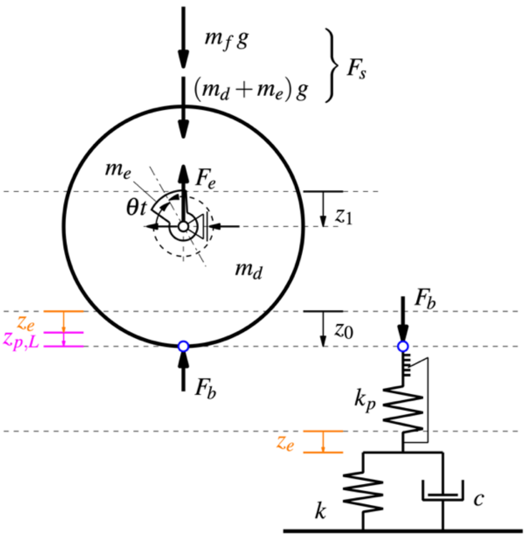


*Figure 1. Free-body diagram of the simplified simulation model at time t during the first load cycle.*

The application of the principle of linear momentum yields the equation of motion for the roller subsystem by means of the resulting soil contact force $F_b$ which comprises the inertia force $F_a$, the static load $F_s$, and the excitation force $F_e$:

$$F_b = -F_a + F_s - F_e = -(m_d + m_e)\ddot{z}_1 + \left(m_d + m_e + m_f\right)g - m_e e \theta^2 \sin(\theta t) \qquad (1)$$

where $m_d$ and $m_e$ are the masses of the drum and the eccentric, $e$ is the eccentricity of the unbalance and $\theta$ is the angular frequency of the excitation.

### 2.2 Modelling of the soil subsystem

The soil subsystem is modelled as a Kelvin-Voigt element, which is extended by an additional spring connected in series (see Figure 1). The calculation of the spring stiffness $k$ and the dashpot coefficient $c$ is based on considerations by Wolf (1994). Therefore, the approximately rectangular contact area between drum and soil with half side lengths $a$ and $b$ is converted into a circle with an equivalent radius, which represents the top surface of a downward unlimited truncated cone. The parameters are defined as (Wolf, 1994):

$$k = \frac{Gb}{1-\nu}\left[3.1\left(\frac{a}{b}\right)^{0.75} + 1.6\right] \qquad (2)$$

$$c = \kappa 4\sqrt{2\rho G\,\frac{1-\nu}{1-2\nu}}\,ab \text{ ... (adapted)} \qquad (3)$$

where $G$, $\rho$, and $\nu$ are the shear modulus, density, and Poisson's ratio of the soil, and $\kappa$ is a factor for increased damping to account for spatial effects. The Kelvin-Voigt model is only able to capture the elastic soil behaviour in the far-field of dynamic compaction. Therefore, an additional elastic spring with stiffness $k_p$ is introduced. The spring deforms proportionally during loading but remains locked otherwise (during unloading and separation) and, therefore, simulates the plastic behaviour in the near-field. The stiffness $k_p$ is estimated by the introduction of a dimensionless condition factor $\varepsilon$ that describes the ratio of elastic to elasto-plastic deformations and provides a relationship between $k_p$ and $k$ (Adam, 1996):

$$\varepsilon = \frac{z_e}{z_e + z_p - z_{p,p}} = \frac{k_p}{k_p + k} \Leftrightarrow k_p = \frac{\varepsilon k}{1-\varepsilon} \qquad (4)$$

where $z_e$ and $z_p$ are the absolute elastic and plastic deformations of the soil, and $z_{p,p}$ is a compensation variable to account for the periodic increase in vertical displacements under cyclic loading. In this paper, a condition factor of $\varepsilon = 0.85$ is defined to simulate the "partial uplift" mode of operation.

### 2.3 Coupling of roller and soil subsystem

The coupling and separation of the two subsystems is characterized by three operating phases – loading, unloading, and separation – which may occur during each period of excitation.

#### 2.3.1 Loading phase

The soil with its position coordinate $z_0$ follows the movement of the drum during the loading phase ($z_0 = z_1$) and the soil contact force $F_b$, as well as its gradient have a positive sign. The spring $k_p$ is active during loading and, therefore, elastic ($z_e$) and relative plastic ($z_{p,L}$) deformations occur. The sum $z_e + z_{p,L}$ is the basis for the calculation of the variable drum contact width (see section 2.4).

The soil contact force for the roller subsystem is given in Equation (1). For the soil subsystem, $F_b$ comprises the forces in the elastic spring ($F_k$) and the viscous dashpot ($F_c$):

$$F_b = F_k + F_c = kz_e + c\dot{z}_e \tag{5}$$

Roller and soil subsystem are coupled by the spring with stiffness $k_p$:

$$F_b = [(z_0 - z_e) - z_{p,p}]k_p + F_{p,p} = z_{p,L}k_p + F_{p,p} \tag{6}$$

The variable $z_{p,L}$ compensates the periodic increase in plastic deformations due to cyclic loading and allows for the calculation of the relative plastic deformations during each load cycle. Therefore, $z_{p,p}$ describes the cumulative pre-deformation of spring $k_p$, which increases by $z_{p,L}$ at each transition from loading to unloading. If the drum does not lose its contact after the unloading phase, a residual preload $F_{p,p}$ of the spring $k_p$ must be taken into account.

The loading phase ends when the soil contact force stops increasing and its gradient is less or equal to zero. The loading phase is always followed by an unloading phase.

### 2.3.2 Unloading phase

During the unloading phase, the soil continues to follow the movement of the drum ($z_0 = z_1$), and Equations (1) and (5) remain applicable for the calculation of the soil contact force. $F_b$ is still positive, while its gradient is negative ($\dot{F}_b \leq 0$). The spring with stiffness $k_p$ is locked ($k_p = \infty$) and therefore only elastic deformations occur.

The unloading phase ends, if the soil contact force starts to increase again without a full unloading and another loading phase begins. In this case, the residual preloading of the spring $k_p$ is taken into account by the variable $F_{p,p}$.

The unloading phase also ends if the soil contact force becomes zero. The separation phase begins since the soil cannot bear tensile forces and the two subsystems move independently from each other.

### 2.3.3 Separation phase

Drum and soil move separately and independently of each other and the soil contact force in Equations (1) and (5) is zero. The soil creeps back towards its initial position during the separation phase. The preload $F_{p,p}$ of the spring $k_p$ is set to zero in case of separation.

The separation phase is always followed by a loading phase.

## 2.4 Variable drum contact width

The contact area between the two subsystems decisively determines the dynamic interaction between drum and soil. Due to the cylindrically curved drum geometry, the contact area is a variable quantity during the loading phase. The drum increasingly penetrates the soil, and the contact width between the subsystems steadily increases, while the length of the load area remains largely constant and equals the length of the drum ($2a$).

In contrast to previous research (Adam, 1996), the presented model enables the consideration of the variable contact width $2b$ during the loading phase. The instantaneous drum contact width is determined using the circular arc segment shown in Figure 2, which is defined by the sagitta $\Delta z$ and the circular chord $s$.

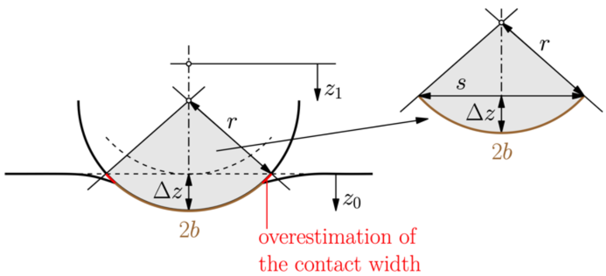


*Figure 2. Calculation of the variable drum contact width.*

With the known drum radius $r$ and the elasto-plastic deformations $\Delta z = z_e + z_{p,L}$, the circular chord $s$ and the circular arc length $2b$ can be calculated according to Equations (7) and (8).

$$s = 2\sqrt{2r\Delta z - \Delta z^2} \tag{7}$$

$$2b = 2r\,arcsin\left(\frac{s}{2r}\right) \tag{8}$$

During the unloading phase, $2b$ is assumed to be constant and corresponds to the value at the end of the loading phase since only elastic deformations occur.

The variable drum contact width results in a variable spring stiffness $k$ and dashpot coefficient $c$ during the loading phase. The definition of $k_p$ by means of a condition factor $\varepsilon$ according to Equation (4) also makes $k_p$ a variable quantity.

# 3 CALCULATIONS AND RESULTS

Selected results from simulations with the presented mechanical roller-soil model are presented for a HAMM H13i single-drum roller. The roller and soil parameters of the simulations are given in Table 1. The soil parameters were selected to ensure the "partial uplift" mode of operation. Ninety revolutions of the eccentric mass were simulated (duration = 3 s), to guarantee a steady state of the simulation.

*Table 1. Roller and soil parameters of the simulation.*

| **Parameter** | **Value** |
|---|---|
| Radius of the drum $r$ | 0.752 m |
| Length of the drum $2a$ | 2.14 m |
| Eccentricity $e$ | 23.21 mm |
| Mass of the frame $m_f$ | 3323.0 kg |
| Mass of the drum $m_d$ | 3722.5 kg |
| Mass of the eccentric $m_e$ | 69.47 kg |
| Excitation frequency $f$ | 30 Hz |
| Shear modulus $G$ | 50 MN/m$^2$ |
| Poisson's ratio $\nu$ | 0.3 |
| Density $\rho$ | 1800 kg/m$^3$ |
| Damping factor $\kappa$ | 4 |
| Condition factor $\varepsilon$ | 0.85 |

Figure 3 shows the calculated soil contact force $F_b$ (black) and its components for four periods of excitation. For the roller subsystem, the contact force is calculated from the inertia force $F_a$ of the vibrating mass shifted upwards by the static axle load $F_s$ (blue) and reduced by the excitation force $F_e$ (green). If the blue and green lines coincide, the soil contact force does not contribute to the inertia force (Equation 1), drum and soil are separated, and the soil contact force becomes zero. The soil contact force shows a recurring pattern for each unbalance revolution, amplitudes and contact times are identical, which means that the roller operates in the "partial uplift" mode.

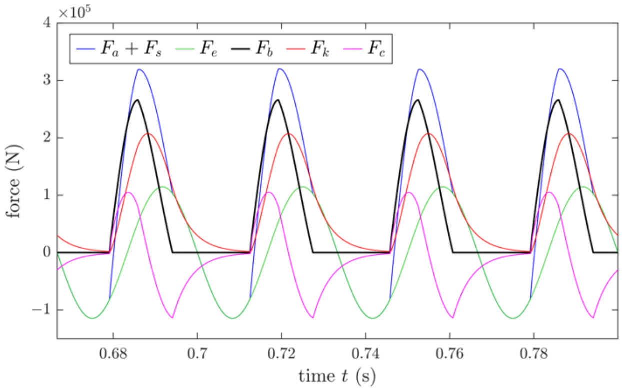


*Figure 3. Soil contact force $F_b$ and its components for the roller and soil subsystem over four periods of excitation.*

The soil contact force $F_b$ can also be calculated for the soil subsystem as sum of the elastic spring force $F_k$ and the force $F_c$ in the dashpot. It becomes zero in the separation phase since the spring and damping forces have the same magnitude.

The force-displacement diagram in Figure 4 shows the relation between the soil contact force $F_b$ (black) and the corrected relative vibration displacement of the drum $z_1$. The curved force-displacement line of the spring force $F_k$ (red) results from the nonlinearities of the compaction process: the variable drum contact area and plastic deformations during the loading phase. The change in contact conditions due to the separation phase results in a pronounced kink in the development of the damping force $F_c$ (magenta).

Additional simulations were performed, considering a constant contact width, only. The results are shown in orange ($2b = 6$ cm) and cyan ($2b = 12$ cm) colour in Figure 4.

A comparison of the force-displacement diagrams with and without variability of the contact width shows that only the described model extension leads to results that are close to reality and comparable with measured data (Adam, 1996).

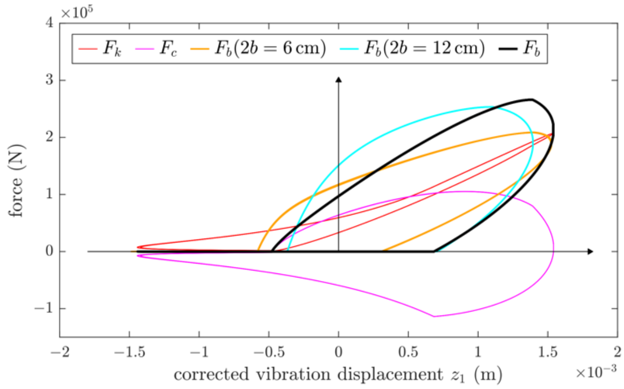


*Figure 4. Force-displacement diagrams for a variable and two constant contact widths in comparison.*

## 4 CONCLUSIONS

The presented semi-analytical model allows to consider the vertical drum motion of a vibratory roller, while considering the variable drum contact width during the loading phase. The theoretical force-displacement diagram in Figure 4 provides the basis for the development of a novel Intelligent Compaction Meter Value (ICMV) for vibratory roller compaction.

## REFERENCES

Adam, D. (1996). *Continuous Compaction Control (CCC) with vibrating rollers*, PhD thesis, TU Wien.

Pistrol, J., Hager, M., Kopf, F., Adam D. (2023). Consideration of the variable contact geometry in roller compaction. *Infrastructures*, 2023 (8): 110. https://doi.org/10.3390/infrastructures8070110

Wolf, J. P. (1994). *Foundation vibration analysis using simple physical models*, 4th ed., PTR Prentice Hall, Upper Saddle River, NJ, USA.